

**Towards the Development of Alanine Serine Cysteine Transporter 2-Selective  
Inhibitors and Molecular Probes to Interrogate Cancer Metabolism**

By

**RONALD TONY ALAN BENNING JR.**

THESIS

Submitted to the Faculty of the  
Graduate School of Vanderbilt University  
in partial fulfillment of the requirements

for the degree of

MASTER OF SCIENCE

in

Chemistry

October 31, 2018

Nashville, Tennessee

Approved:

H. Charles Manning, Ph.D.

Jeffrey N. Johnston, Ph.D.

Steven D. Townsend, Ph.D.

## DEDICATION

This thesis is dedicated to my family: Yolanda Benning (mother), Ronald Benning Sr. (father), Chaz Benning (brother), and Gila M. Rice (daughter). Their ongoing support has helped guide my journey throughout my studies. Born and raised in Trenton, NJ, I am proud to have emerged as a successful model of an underrepresented class of urban city scholars. I am the first member of family to have obtained a bachelor's degree and pursued a graduate education in the natural sciences. I am especially grateful to Dr. John Eugene Sheats (Rider University, emeritus professor) and his commitment to being a mentor and advisor throughout my early exposure to scientific research, through Project S.E.E.D. I also dedicate this achievement to the advisory staff of Rider University's Ronald E. McNair post-baccalaureate program, for surpassing their professional responsibilities and providing support. I am most grateful for my family's role in enabling me to embark on this long endeavor and placing my aspirations before their own.

Special dedication to my dearly departed grandmother.



In loving memory of Ida "Big Ma" Benning  
April 2, 1928 – September 15, 2018

## **ACKNOWLEDGEMENTS**

This work would not have been possible without the financial support of the National Institutes of Health RO1 grant (CA163806), Vanderbilt Center for Molecular Probes TIPS Award, or Vanderbilt University Medical Center institutional funding. I am especially grateful for all research and emotional support from members whom I have worked with. I would like to give special thanks to Dr. Jeffrey N. Johnston for his strong academic presence and guidance throughout my graduate studies in Dr. H. Charles Manning's lab. I would also like to thank, Dr. Michael Nickels and Dr. Michael Schulte, for dedicating their time and commitment to help develop my technical skills. I would like to give special thanks to Dr. H. Charles Manning for giving me the opportunity to work with a talented team of professionals and exposure to a clinically impactful field. I value my time as graduate student in Manning lab, along with all my personal experiences with every individual of the Vanderbilt Institute of Imaging Science and the Center for Molecular Probes.

### Funding Sources:

NIH-RO1-CA163806

Vanderbilt Center for Molecular Probes TIPS Award

Vanderbilt University Medical Center Institutional Funding

## TABLE OF CONTENTS

	Page
<i>DEDICATION</i> .....	<i>i</i>
<i>ACKNOWLEDGEMENTS</i> .....	<i>ii</i>
<i>List of Tables</i> .....	<i>iv</i>
<i>List of Figures</i> .....	<i>v</i>
<i>List of Schemes</i> .....	<i>vi</i>
<b>Chapters</b>	
1. Overview of Key Concepts in Cancer Metabolism .....	1
<i>Introduction</i> .....	1
<i>Glycolysis: Glucose Metabolism in Cancer</i> .....	2
<i>The Role of Glutamine in Cancer Metabolism</i> .....	2
2. Screening Inhibitors of ASCT-2 Mediated Glutamine Uptake .....	6
<i>Introduction</i> .....	6
<i>Experimental</i> .....	7
<i>tert-butyl 4-((2-ethoxy-2-oxoacetamido)methyl)piperidine-1-carboxylate (3)</i> .....	9
<i>2-(((1-(tert-butoxycarbonyl)piperidin-4-yl)methyl)amino)-2-oxoacetic acid (4)</i> .....	9
<i>tert-butyl 4-((2-arylamino)-2-oxoacetamido)methyl)piperidine-1-carboxylate (6a-y)</i> .....	10
<i>N<sup>1</sup>-((1-(cyclopropylsulfonyl)piperidin-4-yl)methyl)-N<sup>2</sup>-aryloxalamide (8a-y)</i> .....	10
<i>2-((3-methylbenzyl)oxy)benzaldehyde (11)</i> .....	12
<i>(S)-2-N-(tert-butoxycarbonyl)amino-4-((2-(3-methylbenzyl)oxy)benzylamino)butanoic acid (13)</i> .	12
<i>Asymmetric 4',4''-N-((2-(3-methylbenzyl)oxy)benzyl)-2-aminobutanoic acids (15a-o)</i> .....	13
<i>ASCT-2 <sup>3</sup>H-Glutamine Uptake Competitive Inhibition Assay</i> .....	13
<i>Results</i> .....	14
<i>Discussion</i> .....	19
<i>Conclusion</i> .....	20
<i>References</i> .....	21
<b>Appendix</b>	
<i>Lewis Structures: Compounds (3-6f)</i> .....	25
<i>Lewis Structures: Compounds (6g-6n)</i> .....	26
<i>Lewis Structures: Compounds (6o-6v)</i> .....	27
<i>Lewis Structures: Compounds (6w-6y)</i> .....	28
<i>Lewis Structures: Compounds (8a-h)</i> .....	29
<i>Lewis Structures: Compounds (8i-q)</i> .....	30
<i>Lewis Structures: Compounds (8q-r)</i> .....	31
<i>NMR Spectra</i> .....	32

## List of Tables

Tables	Page
1. Membrane Bound Transporters.....	4
2. <i>N</i> <sup>1</sup> -(piperidin-4-yl)methyl- <i>N</i> <sup>2</sup> -anilido product yields.....	17
3. ( <i>S</i> )-2-amino-4-((2-((3-methylbenzyl)oxy)benzyl)amino)butyric acid product yields.....	18

## List of Figures

Figures	Page
1. Individually plotted $N^1$ -((1-(cyclopropylsulfonyl)piperidin-4-yl)methyl)- $N^2$ -aryloxalamide screening .....	14
2. Dose response individually plotted, compound 15 derivatives, $n \geq 3$ .....	15

## List of Schemes

Schemes	Page
1. General route to $N^1$ -((1-(cyclopropylsulfonyl)piperidin-4-yl)methyl)- $N^2$ -aryloxalamides (8) .....	8
2. General route to (S)-2-amino-4-((2-((3-methylbenzyl)oxy)benzyl)amino)butyric acids (15).....	11
3. Preparation of $N^1$ -((1-(cyclopropylsulfonyl)piperidin-4-yl)methyl)- $N^2$ -aryloxalamide derivatives .....	17

# CHAPTER 1

## *Overview of Key Concepts in Cancer Metabolism*

### **Introduction**

Cancer is defined as a collection of related diseases that alter cellular function, often causing cells to display atypical traits that lead to benign or malignant growths.<sup>1</sup> Though many of the specific causes of cancer are not yet well-defined, cancer etiology has been linked to changes in gene expression or mutation that include DNA repair, cell division, cell growth, and tumor suppression.<sup>1</sup> For instance, ~40% of colorectal cancer (CRC) patients possess a mutation in *KRAS*, an oncogene that codes for a downstream effector protein involved in EGFR-activated MAPK cascades, which are responsible for cell growth.<sup>2</sup>

There are >100 specific cancer types that have been specified by cell-type and occurrence in various organs.<sup>3</sup> For example, adenocarcinomas are commonly formed by fluid or mucus-producing epithelial cells found on the surfaces of organs.<sup>4</sup> Prior to cancer formation, cells typically undergo abnormal processes called hyperplasia and dysplasia. Hyperplasia is a process when cells over-populate in local areas of organ tissue and appear normal under microscope, whereas the cells appear abnormal in dysplasia. The abnormal cellular growth becomes cancer when cells invade and affect neighboring cells to form primary lesions. In advanced stages of cancer development, cancer cells can migrate to distal regions throughout the body and affect other organ tissues, in a process called metastasis.

Breast, lung, bronchus, prostate and colorectal cancers account for nearly 50% of newly diagnosed cases and lung, colorectal, pancreatic, and breast cancer lead in the most fatalities, according to the National Cancer Institute 2018 statistics.<sup>3, 5</sup> Individualized treatments for high risk cancer patients has become a major priority in clinical research. Much effort has been dedicated to improving early detection and therapeutic intervention by developing new medicinal therapies, identifying new biomarkers associated with tumor progression, and utilizing state-of-the-art imaging modalities towards improving the therapeutic outcomes.



## **Glycolysis: Glucose Metabolism in Cancer**

In 1924, Otto Heinrich Warburg noted that cancer exhibits a cellular dependence on glycolysis in both the absence and presence of oxygen-rich environments; namely the Warburg Effect.<sup>6</sup> The Warburg Effect is accepted as a general principle that accounts for elevated glucose consumption observed in oxygen-deprived tumors that required immense energy to sustain rapid cell division and growth.<sup>6</sup> As tumors progress, cells form dense non-vascularized microenvironments where oxygen becomes limited and restricts the cells to anaerobic conditions, even though conversion of glucose to lactate is less efficient than oxidative phosphorylation in mitochondria (aerobic glycolysis). Furthermore, glycolysis features several convergent intermediates that cancer also leverages in other reversible pathways including single carbon metabolism, glutaminolysis, and nucleotide biosynthesis; evolutionary gateways to feedback and bypass mechanisms.<sup>7</sup> For example, 3-phosphoglycerate is an intermediary precursor in the synthesis of L-phosphoserine that participate in reversible processes featured in the folate cycle, methionine cycle, DNA methylation, and metabolism of other amino acids.

## **The Role of Glutamine in Cancer Metabolism**

L-amino acids exist in fluxional quantities throughout the human body, depending variable demand for key nutrients. Human health affects the body's physiological condition, influencing nutritional supply and demand to impact cells. In cancer, diseased cells exhibit abnormal cellular tendencies that often create disproportionate demands for nutrients. This includes the cellular propensity to selectively over-express (or suppress) key cellular proteins essential to cellular proliferation and respiration, in effort to sustain cell vitality or rapid development. Several studies highlight atypical cellular dependence for glutamine in malignant diseases, including but not limited to colorectal and breast cancers that contribute to high mortality rates.<sup>8-12</sup>

Glutamine (Gln, Q) is a naturally occurring compound, belonging to an endogenous class of alpha-amino acids (*i.e.*, L-Ala, Arg, Asn, Asp, Cys, Gln, Glu, Gly, His, Ile, Leu, Lys, Met, Phe, Pro, Ser, Thr, Trp, Tyr, and Val) that ubiquitously serve as vital substrates in cellular metabolism. These amino acids generally are versatile substrates that are ubiquitously involved in vital cellular processes, including protein

synthesis and cellular respiration. Glutamine stands out as the most abundant amino acids in blood plasma (~500  $\mu\text{M}$ ), accounting for nearly 20% of free amino acids in blood plasma and 40% in muscle.<sup>13-15</sup> In healthy tissues, glutamine is considered a non-essential amino acid, meaning it can be synthesized and consumed in the human body without additional dietary supplement (contrary to essential amino acids).<sup>16</sup> Instances of severe illness and tumor development, like in many cases associated with kidney and gastrointestinal diseases, glutamine exists at deficient levels as an artificial result of insufficient glucose supply and need for nitrogenous substrates.<sup>17-18</sup> In fact, several reports implicate glutamine dependence for tumor growth as evident by reduced cancer cell viability in the absence or depletion of glutamine, despite increased rates of glycolysis.<sup>19-21</sup> Glutamine is utilized as an important substrate in biosynthesis of other essential acids and glucose. Studies have shown glutamine activates rapamycin complex 1 (mTORC1), a major regulator of tumor growth, where glutamine consumption facilitates anabolic growth that is directly linked to oncogenic cancer-Myelomatosis (c-MYC) activation.<sup>17, 21-24</sup>

Glutamine metabolism occurs in all living cells, where glutamine biosynthesis is primarily routed through glutamine synthetase (GLUL1) catalyzed condensation of glutamate and ammonia, pyridoxal phosphate-dependent transamination, and protein degradation. The rationale behind increased glutamine uptake exhibited in cancer is oncogenic reprogramming resulting in a cellular regression to a primitive form to efficiently utilize an abundant fuel source. In addition, c-MYC activation stimulates the up-regulation and activation genes *SLC38A5* (SN2) and *SLC1A5* (ASCT2), two high-affinity glutamine transporters, in a cooperative fashion. Furthermore, the activation of c-MYC enables glutamine transport required for mTORC1 activation, in a collaborative feedback fashion.<sup>23, 25</sup>

In addition, glutamine is a nitrogen donor that plays an essential role as an intermediary constituent in the urea cycle, protein synthesis, nucleotide synthesis, and production of amino acid pools.<sup>26</sup> Ammonia is highly toxic to most living organisms and is typically processed in the liver and kidneys where it is coupled with glutamate, essentially masked in the form of glutamine via PLP-dependent transaminase and GLUL1 enzymes. Since glutamine exists the most abundant amino acid in blood

plasma, its concentration correlates to the amount that is absorbed and secreted by tissues throughout the body<sup>27</sup>.

Table 1. Membrane Bound Transporters

Transporters	Family (# isoforms)	Gene Symbol
Peptides	PEPT1, PEPT2, PTR3, hPT-1, PHT1	SLC15A
Nucleosides	CNTs (3) ENTs (3)	SLC28A SLC29A
Amino Acids	CATs (4), LAT (3) EAATs (5), ASCTs (2) rBAT, 4F2hc GATs (3), BGT, GLYTs (3), TAUT, PROT CT, HTT, DAT1, NAT1, b <sup>(0,+)</sup> AT, ATB	SLC7A SLC1A SLC3A SLC6A SLC6A
Organic Cation	OCTs (3), OCTNs (3)	SLC22A
Organic Anion	OATs (4) OATPs (8)	SLC22A SLC21A
Glucose	SGLTs (3) GLUTs (13)	SLC5A SLC2A
Vitamin	SVCTs (2) Folate (3) SMVT	SLC23A SLC19A SLC5A6
Bile Acids	NTCP, ISBT	SLC10A
Fatty Acids	FATPs (6)	SLC27A
Phosphates	SLC17As (4) SLC34As (2)	SLC17A SLC34A
Monocarboxylic Acids	MCTs (6)	SLC16A
Bicarbonates	SBC2, HNBC1	SLC4A
ABC	ABCAs (12), ABCBs (10), ABCCs (12) ABCDs (8), ABCEs (1), ABCFs (13) ABCGs (6)	ABC

Table 1 was adapted from He, L.; Vasiliou, K.; Nebert, D. W., Analysis and update of the human solute carrier (SLC) gene superfamily. Human Genomics 2009, 3 (2), 195<sup>28</sup>

There exist over 400 membrane bound transporter proteins that have been organized into 65 classes, with the family of solute carrier (SLC) family. Table 1 summarizes several general classes of SLC gene encoded membrane bound transporters found throughout human tissue. Alanine-Serine-Cysteine Transporter (gene symbol: *SLC1A*) is an evolutionarily redundant amino acid transporter protein belonging to a class of solute carrier proteins (1A), which include: ASCT-1 (*SLC1A4*), ASCT-2 (*SLC1A5*), and excitatory amino acid transporters (EAATs).<sup>27, 29</sup> Interestingly, ASCT-2 has been identified as a high affinity glutamine transporter corresponding with elevated expression level in various cancers, despite similarities in genetic sequences within its family of amino acid transporters. Glutamine can also be shuttled by other

membrane bound transporters (*i.e.* LAT1, SNAT1, SN2), however ASCT-2 expression and glutamine transport activity are relatively greater in comparison to other surface bound transporters in various cancer cells.<sup>30-32</sup>

Neutral amino acid transport, *via* ASCT2, is thought to involve binding of three Na<sup>+</sup> ions and possesses a highly conserved zwitterionic recognition site that facilitates amino acid transport.<sup>27</sup> Given glutamine's critical role and ASCT-2 high expression levels exhibited in high profile cancers, ASCT-2 represents an attractive target for development of new therapies.

## CHAPTER 2

### *Screening Inhibitors of ASCT-2 Mediated Glutamine Uptake*

#### Introduction

ASCT-2 mediated glutamine (GLN) uptake in cancer has recently been elucidated as critical proponent of cellular metabolism and rapid tumor progression.<sup>33</sup> To date, only a few compounds have been reported with modest selectivity in targeting ASCT-2. In 2004,  $\gamma$ -glutamyl-para-nitroanilide (GPNA) was reported as an inhibitor of ASCT-2 with modest selectivity ( $IC_{50}$ :  $\sim 1$  mM), emerging from a series of gamma-*N*-anilido glutamine analogs, which was extended in a brief SAR study by Schulte and co-workers to provide additional insight to the lesser known ASCT-2 binding domain.<sup>34-35</sup> Schulte and co-workers demonstrated selective inhibition of ASCT-2 in human HEK293 cell lines, with 2-amino-4-bis((3-methylbenzyloxy)benzylamino)butanoic acid (V9302,  $IC_{50}$ :  $9.6 \mu\text{M}$ ).<sup>36-37</sup>

In preliminary work relevant to this thesis, computational software (PyMOL)<sup>38</sup> was utilized to perform iterative virtual screens as a qualitative guide towards identifying novel scaffolds tailored for ASCT-2's (PDB: 2NWW) binding pocket. Upon qualitative evaluation of several structural poses of general molecular motifs using in-silico modeling, *N*-methylpiperidin-4-ylloxalamides were sought after in early exploration of novel molecular templates with a complimentary fit with respect to ASCT-2's binding domain. It was hypothesized that the *N*-methylpiperidin-4-ylloxalamide moiety offers a suitable binding platform to introduce derivatives to develop efficacious inhibitors. Though exploitation of oxalamides as ASCT-2 inhibitors was unprecedented, reports on its utility in stabilizing cationic coordination complexes and reduced susceptibility to rapid hydrolysis reinforced its potential as biologically-relevant motifs.<sup>39</sup> Based upon these studies, biological screening and synthesis of new asymmetric derivatives were sought to be iteratively optimized with medicinal chemistry. In this work, oxalamides were initially pursued to identify novel scaffolds inhibitors, while synthesis of a novel series of asymmetric 4-*N*-substituted- $\alpha$ -amino-2-aminobutanoic acids was exploited in a collective effort to develop new therapeutic to target ASCT-2.

## Experimental

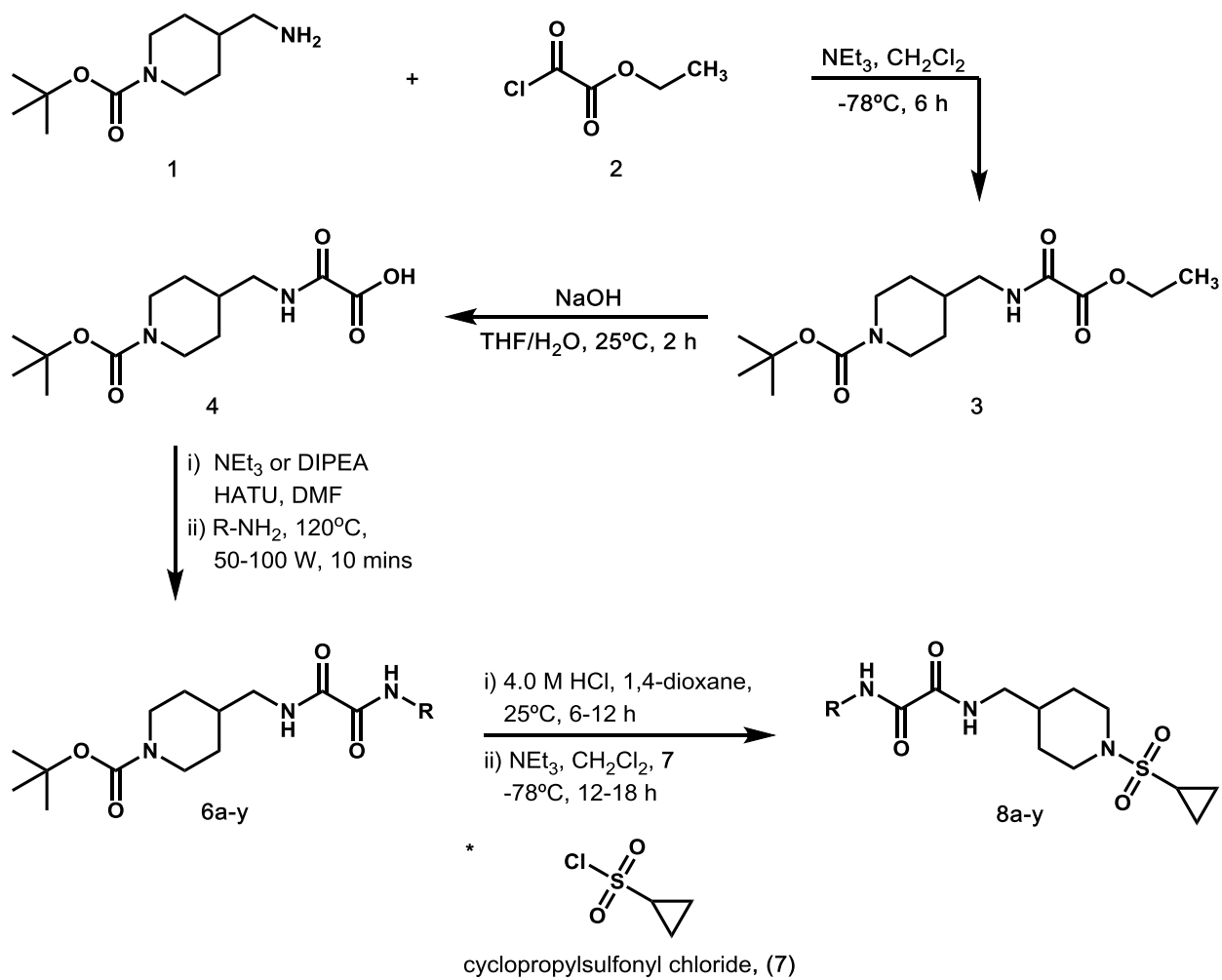
In this study, several *N*-cyclopropylsulfonamidopiperidinyloxalamides **8** were synthesized in effort to evaluate a novel scaffold with the potential to selectively inhibit ASCT-2 mediated glutamine uptake. Scheme 1 outlines the amidation of *tert*-butyl 4-(aminomethyl)piperidine-1-carboxylate **1** (97%, Oakwood Chemicals, Item#: 011389) with ethyl oxalyl chloride **2** (>98%, Oakwood Chemicals, Item#: 024489) yielding *tert*-butyl 4-((2-ethoxy-2-oxoacetamido)methyl)piperidine-1-carboxylate **3**, which is readily converted to 2-(((1-(*tert*-butoxycarbonyl)piperidin-4-yl)methyl)amino)-2-oxoacetic acid **4** *via* treatment with alkaline hydroxide solution.

HATU<sup>1</sup> assisted *N*-coupling methods were employed to prepare *tert*-butyl 4-((2-arylamino)-2-oxoacetamido)methyl)piperidine-1-carboxylate **6**. Removal of *N*-Boc protecting group followed by subsequent addition of cyclopropylsulfonyl chloride **7** yielding *N*<sup>1</sup>-((1-(cyclopropylsulfonyl)piperidin-4-yl)methyl)-*N*<sup>2</sup>-aryloxalamide **8**, in the final step.

---

<sup>1</sup> HATU - hexafluorophosphateazabenzotriazole tetramethyluronium hexafluorophosphate

Scheme 1. General route to  $N^1$ -((1-(cyclopropylsulfonyl)piperidin-4-yl)methyl)- $N^2$ -aryloxalamides (**8**)



**tert-butyl 4-((2-ethoxy-2-oxoacetamido)methyl)piperidine-1-carboxylate (3):** To a flame dried 250 mL round bottom flask, equipped with magnetic stir bar, tert-butyl 4-(aminomethyl)piperidine-1-carboxylate 1 (3.0 g, 14.0 mmol) was dissolved in dichloromethane (70 mL). Solution was cooled to 0°C in ice bath, prior to adding triethylamine (2.0 mL, 14.0 mmol). Reaction mixture was allowed to equilibrate for 5-10 minutes. To stirring mixture, ethyl oxalyl chloride 2 (1.72 mL, 15.4 mmol) was added dropwise (ca. 15 minutes). Reaction was allowed to stir and gradually warm to 25°C, over 6 hours. Reaction mixture was then subjected to an evaporative workup to give a crude yellow oil. Product was purified by flash column chromatography (silica gel 60, 1:3 ethyl acetate/hexanes) to give a colorless oil (4.05 g, 92%).

**2-(((1-(tert-butoxycarbonyl)piperidin-4-yl)methyl)amino)-2-oxoacetic acid (4):** To a 250 mL Erlenmeyer flask, equipped with stir bar, tert-butyl 4-((2-ethoxy-2-oxoacetamido)methyl)piperidine-1-carboxylate 3 (4.02 g, 12.8 mmol) was dissolved in 2-methyl tetrahydrofuran (70 mL). Solution was then treated with 1.0 M NaOH (70 mL) and vigorously stirred for 1 h period, at ambient temperature. The pH was adjusted 1-2 with 1.0 M KHSO<sub>4</sub>. Reaction mixture was diluted and extracted with ethyl acetate (3x100 mL). Organic layers were combined, dried over Na<sub>2</sub>SO<sub>4</sub>, and filtered. Organic layer was then concentrated in-vacuo yielding an off-white solid as crude product. Product was precipitated in (1:1:5) chloroform, diethyl ether, and hexanes yielding a colorless solid (3.37 g, 92%).

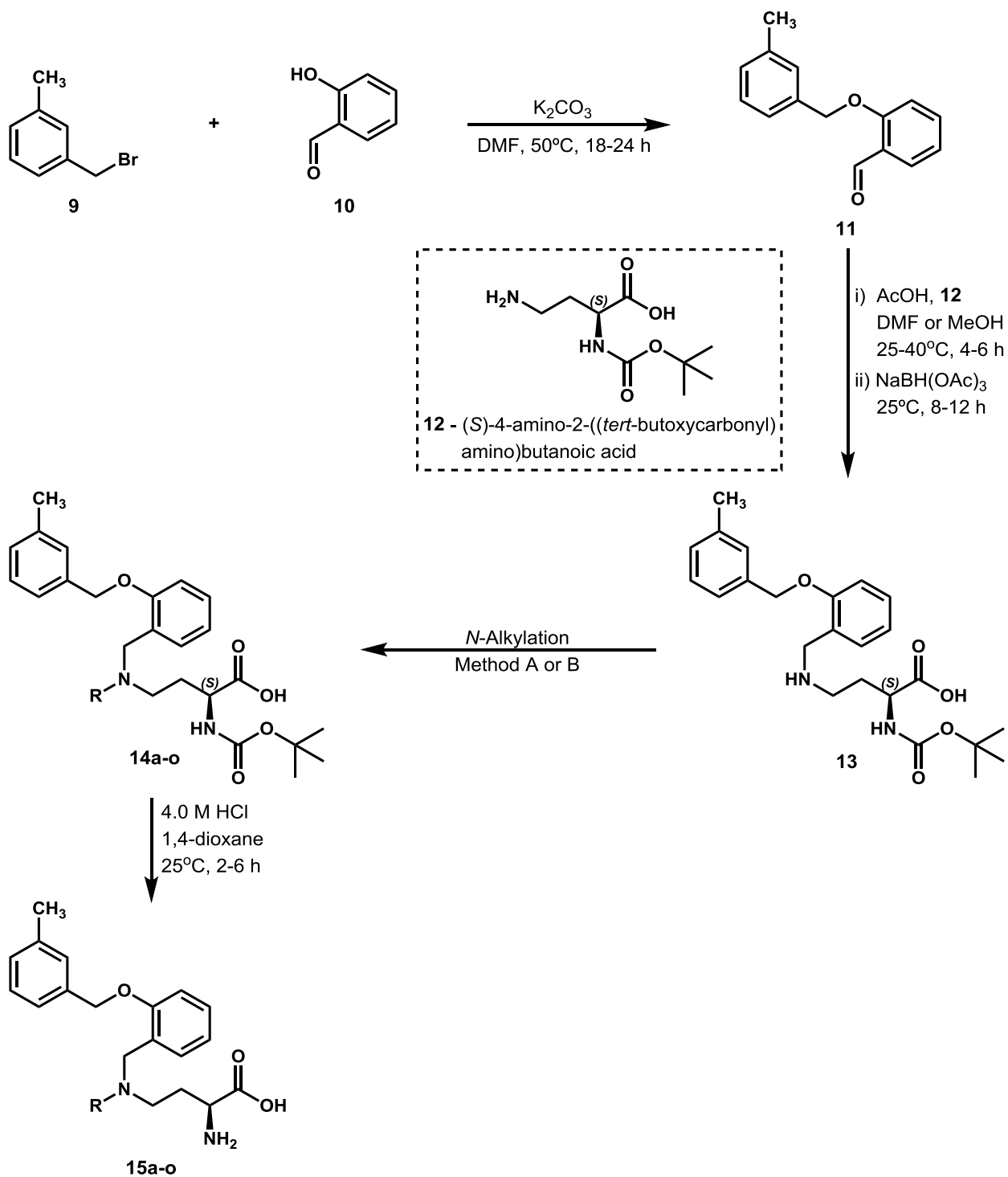


**tert-butyl 4-((2-arylamino)-2-oxoacetamido)methyl)piperidine-1-carboxylate (6a-y):**

To an oven dried 2-5 mL microwave reaction vial (Biotage), equipped with stir bar, 2-(((1-(*tert*-butoxycarbonyl)piperidin-4-yl)methyl)amino)-2-oxoacetic acid 4 (50.0 mg, 0.175 mmol) and diisopropylethylamine (120.0  $\mu$ L, 0.700 mmol) were dissolved in *N,N*-dimethylformamide (2.0 mL). Solution was allowed to equilibrate (ca. 15-20 min) prior to adding hexafluorophosphateazabenzotriazole tetramethyluronium hexafluorophosphate (70.0 mg, 0.184 mmol). Reaction contents were stirred (ca. 20 min) prior to addition of aniline (0.193 mmol). Reaction vial was sealed and subjected to microwave irradiation (120°C, 50-100W) for 10 minutes. Reaction mixture was diluted with ethyl acetate (20 mL), then treated with 1.0 M HCl (1 mL). Organic layer was washed with distilled H<sub>2</sub>O (2 x 5 mL), then brine (5 mL). Organic layer was then dried over Na<sub>2</sub>SO<sub>4</sub> and filtered through Celite®. Crude product was concentrated in-vacuo and purified by flash column chromatography (silica gel 60, 20-50% ethyl acetate/hexanes).

**N<sup>1</sup>-((1-(cyclopropylsulfonyl)piperidin-4-yl)methyl)-N<sup>2</sup>-aryloxalamide (8a-y):** To a flame dried 5 mL round bottom flask, equipped with stir bar, tert-butyl 4-((2-arylamino)-2-oxoacetamido)methyl)piperidine-1-carboxylate 6 (0.036 mmol) was treated with 4.0 M HCl in dioxane solution (45.0  $\mu$ L, 0.18 mmol). Reaction was allowed to stir at 25°C, for 2 h. Reaction mixture was diluted with diethyl ether (2.0 mL) and concentrated in-vacuo. Crude product was then dissolved in dichloromethane (0.4 mL) and cooled to -70°C. Triethylamine (10.0  $\mu$ L, 0.0717 mmol) was added to stirring solution, while temperature was maintained at -70°C. Cyclopropylsulfonylchloride 7 (5.0  $\mu$ L, 0.043 mmol) was then added, and reaction was allowed to stir and gradually warm to 25°C over 2-4 h period. Reaction mix was then diluted with dichloromethane (2.0 mL) and concentrated in-vacuo. Product was then purified by flash column chromatography (silica gel 60, 30-50% ethyl acetate/hexanes).

Scheme 2. General route to (S)-2-amino-4-((2-((3-methylbenzyl)oxy)benzyl)amino)butyric acids (**15**)



N-Alkylation methods: A): 0.2-0.5 M (**13**), aldehyde (1.1 eq), AcOH (1-1.3 eq), NaBH(OAc)<sub>3</sub> (1.5 eq), 1,2-DCE or CH<sub>2</sub>Cl<sub>2</sub>, 25-40°C, 18-24 h; B) 0.1-0.5 M (**13**), 37% formaldehyde in H<sub>2</sub>O/10% MeOH, 88% formic acid, 0-25°C, 2 h

**2-((3-methylbenzyl)oxy)benzaldehyde (11):** To a flame dried 500 mL round bottom flask, equipped with stir bar, was added potassium carbonate (9.16 g, 66.3 mmol) and tetrabutylammonium iodide (1.63 g, 4.41 mmol) under inert atmosphere. Salicylaldehyde (4.71 mL, 44.2 mmol) was added to reaction flask and contents were then suspended in *N,N*-dimethylformamide (220 mL). 3-methylbenzylbromide (6.56 mL, 48.6 mmol) was transferred to flask, and reaction was heated to 50°C for 18 h. Reaction was cooled to room temperature and transferred to 500 mL separatory funnel, and extracted with diethyl ether (200 mL). Organic layer was washed with distilled water (3 x 250 mL), 1.0 M HCl (3 x 75 mL), followed by another portion of distilled water (100 mL). Organic layer was treated with solutions of saturated NaHCO<sub>3</sub> (aq). Saturated NH<sub>4</sub>Cl (aq) was used to neutralize prior to washing organic layer with 1.0 M Na<sub>2</sub>S<sub>2</sub>O<sub>3</sub> then brine. Organic layer was dried over Na<sub>2</sub>SO<sub>4</sub>, filtered through Celite®, and concentrated in-vacuo to give a crude yellow to colorless oil. Product was then purified by flash column chromatography (silica gel 60, 0-20% ethyl acetate/hexanes) yielding a colorless oil (8.5 g, 85%).

**(S)-2-N-(tert-butoxycarbonyl)amino-4-((2-(3-methylbenzyl)oxy)benzylamino)butanoic acid (13):** To an oven dried 50 mL round bottom flask, equipped with stir bar, (S)-4-amino-2-((tert-butoxycarbonyl)amino)butanoic acid 12 (767 mg, 3.51 mmol) was dissolved in methanol (20 mL), at 25°C. 2-((3-methylbenzyl)oxy)benzaldehyde 11 (794 mg, 3.51 mmol) and glacial acetic acid (261 µL, 4.56 mmol) were transferred to reaction flask. Reaction was warmed and set to stir at 40°C, for 4-6 h. Reaction was cooled to 25°C and sodium triacetoxyborohydride (1.12 g, 5.27 mmol) was then added to reaction flask as solid. Reaction was set to stir at 25°C, for 6-12 h. Reaction mixture was quenched with several drops of 1.0 M HCl, reaction solvent was removed, and crude product was reconstituted in dichloromethane (100 mL). Organic layer was washed with distilled water (2 x 50 mL), and aqueous phase was then extracted with dichloromethane (3 x 20 mL). Organic layers were combined, filtered through Celite®, and concentrated in-vacuo. Product was then purified by flash column chromatography (silica gel 60, 0-10% methanol/dichloromethane) yielding a colorless solid (1.34 g, 89%)

### **Asymmetric 4',4''-N-((2-(3-methylbenzyl)oxy)benzyl)-2-aminobutanoic acids (15a-o)**

To a flame dried 25 mL round bottom flask, equipped with stir bar, (*S*)-2-*N*-(*t*-butoxycarbonyl)amino-4-((2-(3-methylbenzyl)oxy)benzylamino)butanoic acid **13** (100 mg, 0.233 mmol) was dissolved in 1,2-dichloroethane (1 mL). Glacial acetic acid was added to solution, followed by aldehyde (0.256 mmol). Reaction flask was set to stir heated to 40°C. After 1 h, sodium triacetoxyborohydride (74.1 mg, 0.350 mmol) was added and reaction was allowed to proceed for additional 16 h. Reaction mixture was quenched with 1.0 M HCl and extracted with dichloromethane (3 x 5 mL). Organic layers were combined, dried over Na<sub>2</sub>SO<sub>4</sub>, and filtered through Celite®. Crude product was concentrated in-vacuo and treated 4.0 M HCl (11.7 mL, 4.66 mmol) in dioxane. Reaction mixture was stirred at 25°C, for 6 h. Reaction solvent was removed in-vacuo and re-constituted in diethyl ether (3 x 10 mL). A portion of diethyl ether (5 mL) was added to crude product and decanted to yield off-white to colorless solid. No further purification was required.

**ASCT-2 <sup>3</sup>H-Glutamine Uptake Competitive Inhibition Assay** Buffer Solution: 137 mM NaCl, 5.1 mM KCl, 1.1 mM CaCl<sub>2</sub>, 0.77 mM KH<sub>2</sub>PO<sub>4</sub>, 0.71 mM MgSO<sub>4</sub>, 10 mM D-glucose, 10 mM HEPES), pH: 6.0. Cells were plated in 96-well plate coated with poly-D-lysine prior plating HEK293 cells at a density of 35,000 cells per well. Cells were grown to 80% confluence and washed with buffer. Cells were then incubated in buffer solution for a two-day period at 37°C. Assays were run by administration of concomitant dose of 500 nM <sup>3</sup>H-glutamine + 5 mM BCH and 100 mM compound diluted with buffer to desired concentration. Cells were then incubated for 5 minutes, washed with buffer, and then analyzed on scintillation counter to quantify gamma radiation from presence of cellular <sup>3</sup>H-glutamine.

## Results

In-vitro competitive  $^3\text{H}$ -glutamine uptake inhibition assays were performed by administering a concomitant dose of test compound prepared from a 100 mM stock in molecular biology grade DMSO. Test concentrations were prepared by serial dilutions with assay buffer and 500 nM  $^3\text{H}$ -glutamine (5 mM BCH in buffer). Vehicles (controls) included HEK293 cells + buffer (137 mM NaCl, 5.1 mM KCl, 1.1 mM  $\text{CaCl}_2$ , 0.77 mM  $\text{KH}_2\text{PO}_4$ , 0.71 mM  $\text{MgSO}_4$ , 10 mM *D*-glucose, 10 mM HEPES), adjusted to pH: 6.0. Blank samples included buffer only. Cells plated in 96 well plate with cell density: 35,000 cells per well. Assays were run using the following test concentrations 1 mM, 500  $\mu\text{M}$ , 250  $\mu\text{M}$  (n=3 biological replicates).

Several oxalamide derivatives (8a, 8b, 8d, 8e, 8f, and 8g) were selected for screening competitive inhibition in  $^3\text{H}$ -glutamine uptake assay (Cell line: human HEK293). Dose responses appeared flat for each entry, with little activity shown with compounds **8b** and **8g**, 2-chlorophenyloxalamide and 2-morpholinophenyloxalamide derivatives respectively.

Figure 1. Individually plotted  $N^1$ -((1-(cyclopropylsulfonyl)piperidin-4-yl)methyl)- $N^2$ -aryloxalamide screening

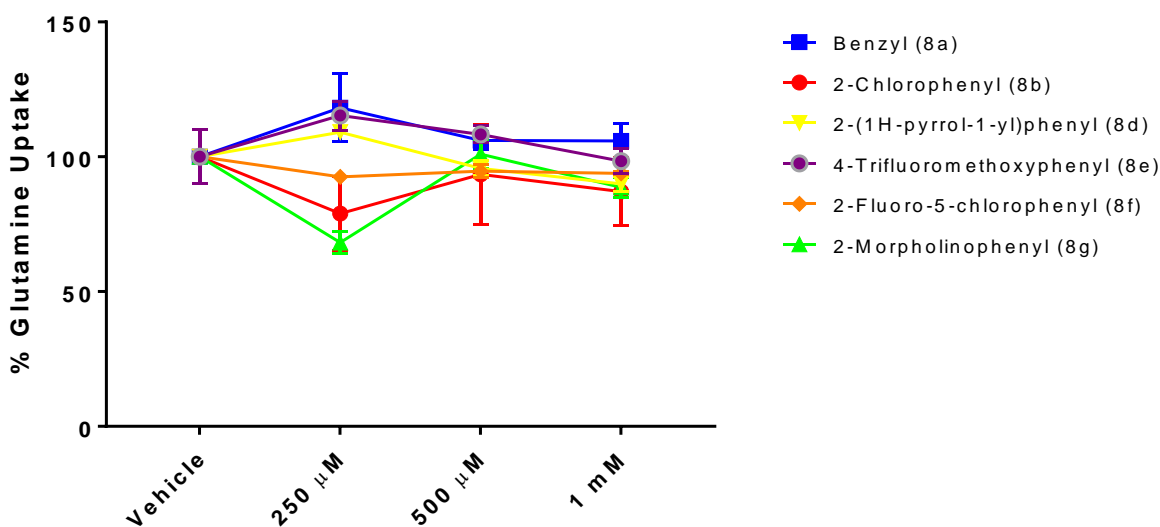
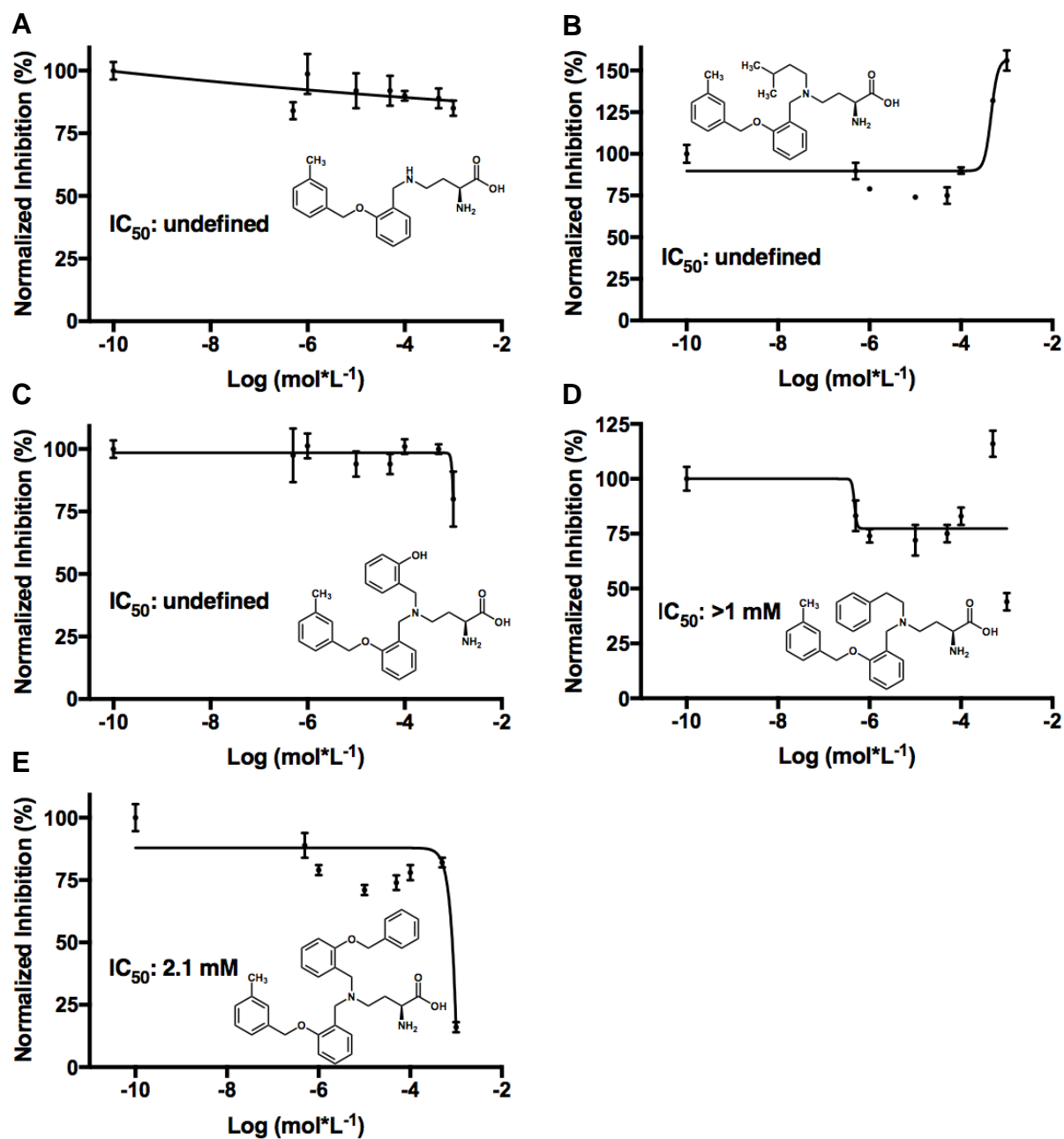


Fig. 1 shows normalized dose response curves for test concentration measured against  $^3\text{H}$ -glutamine uptake, Compounds: A) **8a**; B) **8b**; C) **8d**; D) **8e**; E) **8f**; F) **8g**.

Similar to screening oxalamide derivatives, several compounds from the asymmetric series of  $\alpha$ -aminobutyric acids were evaluated as glutamine analogs, in an analogous fashion. Compound **15** derivatives were plotted as a function of test concentrations against normalized  $^3\text{H}$ -glutamine uptake in HEK293 cells. These derivatives were tested at concentrations: 500 nM, 1  $\mu\text{M}$ , 10  $\mu\text{M}$ , 50  $\mu\text{M}$ , 100  $\mu\text{M}$ , 500  $\mu\text{M}$  and 1 mM.

Figure 2. Dose response individually plotted, compound **15** derivatives,  $n \geq 3$



Preparation of oxamic acid **4** gave reproducible yields within 80-92% (up to 3.0 gram scale). The ethyl ester **3** could also be isolated and purified, however it was found that this was not practical given its susceptibility to hydrolyze to **4**, under ambient conditions. The major byproduct produced from this synthesis is predominantly the *N*-Boc-deprotected amine product, which is an intermediate in subsequent reactions. No significant presence of by-products or side reactions was observed. Although, it was found that subjecting compound **3** to strong alkaline solutions for extended reaction times, promoted formation of unknown product with a molecular mass fragment corresponding to the carbamic acid adduct (only observed on ESI-LC/MS(+), low resolution).

HATU assisted *N*-coupling methods were employed to afford compounds **6** (see Scheme 3). Though HATU assisted coupling reactions appeared to produce a broad range of product yields, these results are reflective of non-optimized conditions (refer to Table 2). At this time, priority was focused on obtaining sufficient quantities of test compounds for biological screening assays. Product yields did not significantly vary when conventional or microwave heating was applied, based on experimental observation. In cases where no desired product was obtained, only un-identifiable by-products or recoverable starting materials were observed.

Successful coupling reactions affording *N*-Boc-piperidinyloxalamide **6**, compounds were then de-protected and conjugated with cyclopropylsulfonyl chloride **7** (Schemes 2 and 3). All corresponding yields are tabulated in Table 2. Products **8** were purified, isolated, and stored at -20°C, until compounds were ready for biological screening. In addition to preparing oxalamides, (*S*)- $\alpha$ -amino- $\gamma$ -butyric acids were synthesized and evaluated as glutamine analogs for selective ASCT-2 inhibition. Derivatives of compound **15** were generally prepared by electrophilic addition to (*S*)-2-*N*-(*t*-butoxycarbonyl)amino-4-((2-(3-methylbenzyl)oxy)benzylamino)butanoic acid **13** by reductive amination or alkyl halide displacement conditions, followed by *N*-Boc de-protection to yield compounds **15**.

Scheme 3. Preparation of *N*<sup>1</sup>-((1-(cyclopropylsulfonyl)piperidin-4-yl)methyl)-*N*<sup>2</sup>-aryloxalamide derivatives

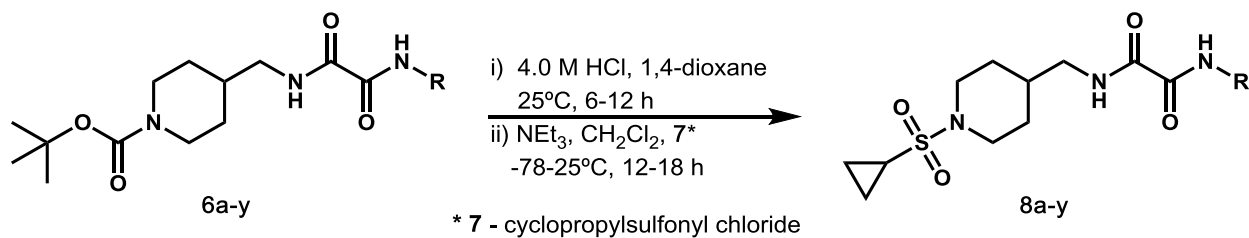


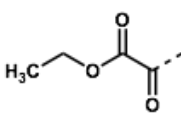
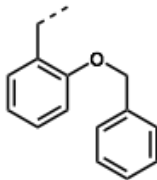
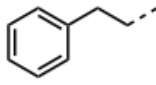
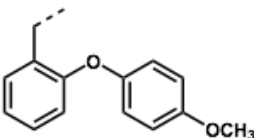
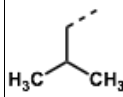
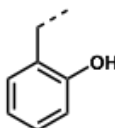
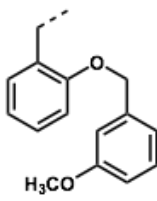
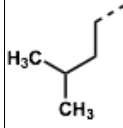
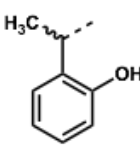
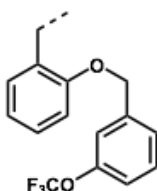
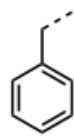
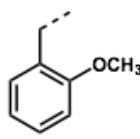
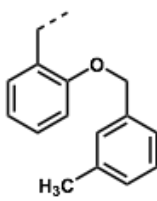
Table 2. *N*<sup>1</sup>-(piperidin-4-yl)methyl)-*N*<sup>2</sup>-anilido product yields (6: N-Boc; 8: N-cyclopropylsulfonyl)

R	Yield	R	Yield	R	Yield	R	Yield
	6a: 97% 8a: 20%		6h: 14% 8h: 53%		6o: 23% 8o: 0%		6v: 19% 8v: n/a
	6b: 97% 8b: 26%		6i: 19% 8i: 28%		6p: 96% 8p: 0%		6w: 15% 8w: n/a
	6c: 58% 8c: 58%		6j: 13% 8j: 18%		6q: 89% 8q: 0%		6x: 14% 8x: n/a
	6d: 98% 8d: 31%		6k: 31% 8k: 6%		6r: 0% 8r: n/a		6y: 7% 8y: n/a
	6e: 77% 8e: 32%		6l: 12% 8l: 11%		6s: 0% 8s: n/a		
	6f: 62% 8f: 42%		6m: 36% 8m: 0%		6t: 34% 8t: n/a		
	6g: 87% 8g: 21%		6n: 6% 8n: 0%		6u: 25% 8u: n/a		

"0%" indicates attempted reactions where no desired product was able to be isolated.  
 "n/a" indicates reaction was not carried out due to insufficient quantity of N-Boc product.



Table 3. (S)-2-amino-4-((2-((3-methylbenzyl)oxy)benzyl)amino)butyric acid product yields

R	Yield	R	Yield	R	Yield
H	13: 72% 15a: 76%		14f: 33% 15f: n/a		14k: 27% 15k: 50%
CH <sub>3</sub>	14b: 87% 15b: 65%		14g: 23% 15g: 55%		14l: n/a 15l: n/a
	14c: 55% 15c: 45%		14h: 20% 15h: 72%		14m: n/a 15m: n/a
	14d: 82% 15d: 70%		14i: 0% 15i: n/a		14n: n/a 15n: n/a
	14e: 50% 15e: 81%		14j: 13% 15j: 20%		14o: n/a 15o: n/a

## Discussion

In 2018, Scopelliti and co-workers evaluated mutagenic effects on substrate selectivity and binding affinity in comparing neutral and acidic amino acid transporters; excitatory amino acid transporters (EAAT1-3), ASCT-1, ASCT-2, and prokaryotic ASCT homologs (Glt<sub>PH</sub>). It was found that ASCT-2-S481T and ASCT-2-C482T mutations (located in the TM8 helical segment of binding domain) caused ASCT-2's binding profile to altered from selective neutral to acidic amino acid transport.<sup>30</sup> Furthermore, S481 and C482 residues could be attributed to ASCT-2 high affinity and selectivity for L-glutamine; coinciding with the efficacy of glutamyl-based inhibitors previously established by Schulte and Esslinger.

New insight into targeting ASCT-2 as a clinically impactful biomarker, motivated further pursuit toward a new class of efficacious and selective ASCT-2 inhibitors. During the developmental stage of research related to this thesis, it was hypothesized that substrate recognition was promoted hydrogen bond donor S481 and C482 residues located in ASCT-2 binding site. Thus, conservation of an  $\alpha$ -amino carboxylate terminus was considered in molecular design. It was further hypothesized that introducing hydrophobic and rotatable bonds could induce a good fit in remote sites of ASCT-2's lipophilic binding domain. For this reason, branched derivatives of the asymmetric 4',4''-N-((2-(3-methylbenzyl)oxy)benzyl)-2-aminobutanoic acids were expected to outperform truncated aliphatic analogs.

Derivatives outlined in Tables 2 and 3 can be interpreted as structural hypotheses in the evaluation of aromatic, aliphatic, branched, and heteroatom analogs. Aromatic and branched compounds were pursued to interrogate the spatial tolerance of ASCT-2 binding domain. Bis((2-(3-methylbenzyl)oxy)benzyl)-2-aminobutanoic acid (V9302) was utilized as a structural template. One objective was to determine if there were any symmetry requirements bifurcated (2-aryloxy)benzyl-2-aminobutanoic acids to elicit a potent pharmacological response. The strategy chosen to address this question was to truncate distal portions of one (2-aryloxy)benzyl arm. Interestingly, disconnection of one methyl moiety from the native V9302 structure appears to significantly reduce its binding affinity.

## Conclusion

Though oxalamides did not appear to inhibit glutamine uptake, these compounds were not immediately dismissed as inactive compounds. Interestingly, compounds **8a**, **8d**, and **8e** appeared to increase glutamine uptake at low concentrations, which would suggest positive modulation of ASCT-2 to activate glutamine transport. Data suggested piperidinylsulfonyloxalamides did not appear to significantly inhibit glutamine uptake in HEK293 cells, instead they may exhibit features of substrates for ASCT-2. Oxalamides were no longer pursued as pharmacological inhibitors for ASCT-2. Attention was then focused on 2-amino-4-(aryloxybenzylamino)butyric acids derivatives **15**, which revealed promising potential as efficacious inhibitors. As portrayed in Figure 4, inhibition was observed with the benzyloxy and homobenzyl analogs (**15g** and **15k**, respectively). However, the aliphatic and truncated aryl derivatives did not elicit significant inhibition. This data would suggest that bis-substituted 3-methylbenzyloxy derivative ranks superior, though it can be argued that only one methyl may be critical for SAR and optimal docking in the orthosteric site of ASCT-2. These findings support previously proposed mechanisms of zwitterionic recognition followed by molecular rotations to accommodate distal lipophilic regions of substrate. ASCT-2 binding site may be receptive to various substrate types; though inhibition may be strictly conserved to a combination of zwitterionic recognition causing specific conformational changes in lipophilic binding region to induce gated-transport. Nonetheless, this investigation has put forth a precedence to further evaluate new hydrophobic derivatives and potentiates insertion of F-18 or C-11 analogs for PET imaging.

## References

1. Osgood, C. L.; Tantawy, M. N.; Maloney, N.; Madaj, Z. B.; Peck, A.; Boguslawski, E.; Jess, J.; Buck, J.; Winn, M. E.; Manning, H. C.; Grohar, P. J., 18F-FLT Positron Emission Tomography (PET) is a Pharmacodynamic Marker for EWS-FLI1 Activity and Ewing Sarcoma. *Sci Rep* **2016**, *6*, 33926.
2. Ewing, I.; Hurley, J. J.; Josephides, E.; Millar, A., The molecular genetics of colorectal cancer. *Frontline Gastroenterology* **2014**, *5* (1), 26-30.
3. Institute, N. C. What is Cancer? <https://www.cancer.gov/about-cancer/understanding/what-is-cancer> (accessed February 09, 2015).
4. Saksena, R.; Gao, C.; Wicox, M.; de Mel, A., Tubular organ epithelialisation. *Journal of Tissue Engineering* **2016**, *7*, 2041731416683950.
5. Institute, N. C. Cancer Stat Facts: Lung and Bronchus Cancer. <https://seer.cancer.gov/statfacts/html/lungb.html>.
6. Vander Heiden, M. G.; Cantley, L. C.; Thompson, C. B., Understanding the Warburg Effect: The Metabolic Requirements of Cell Proliferation. *Science* **2009**, *324*, 1029-1033.
7. Yang, L.; Venneti, S.; Nagrath, D., Glutaminolysis: A Hallmark of Cancer Metabolism. *Annual Review of Biomedical Engineering* **2017**, *19* (1), 163-194.
8. Huang, F.; Zhang, Q.; Ma, H.; Lv, Q.; Zhang, T., Expression of glutaminase is upregulated in colorectal cancer and of clinical significance. *International Journal of Clinical and Experimental Pathology* **2014**, *7* (3), 1093-1100.
9. Reitzer, L. J.; Wice, B. M.; Kennell, D., Evidence that glutamine, not sugar, is the major energy source for cultured HeLa cells. *Journal of Biological Chemistry* **1979**, *254* (8), 2669-2676.
10. Moses, M. A.; Neckers, L., The GLU that holds cancer together: targeting GLUTamine transporters in breast cancer. *Cancer Cell* **2015**, *27* (3), 317-9.
11. van der Hulst, R. R.; von Meyenfeldt, M. F.; Soeters, P. B., Glutamine: an essential amino acid for the gut. *Nutrition (Burbank, Los Angeles County, Calif.)* **1996**, *12* (11-12 Suppl), S78-81.

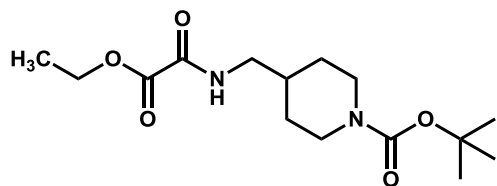
12. Klimberg, V. S.; Souba, W. W., The importance of intestinal glutamine metabolism in maintaining a healthy gastrointestinal tract and supporting the body's response to injury and illness. *Surgery annual* **1990**, *22*, 61-76.
13. Mayers, J. R.; Vander Heiden, M. G., Famine versus feast: understanding the metabolism of tumors in vivo. *Trends in biochemical sciences* **2015**, *40* (3), 130-140.
14. Coster, J.; McCauley, R.; Hall, J., Glutamine: metabolism and application in nutrition support. *Asia Pacific journal of clinical nutrition* **2004**, *13* (1), 25-31.
15. Bergström, J.; Fürst, P.; Norée, L. O.; Vinnars, E., Intracellular free amino acid concentration in human muscle tissue. *Journal of Applied Physiology* **1974**, *36* (6), 693-697.
16. Hall, J. C.; Heel, K.; McCauley, R., Glutamine. *The British journal of surgery* **1996**, *83* (3), 305-12.
17. Wise, D. R.; Thompson, C. B., Glutamine Addiction: A New Therapeutic Target in Cancer. *Trends in biochemical sciences* **2010**, *35* (8), 427-433.
18. Kelly, D.; Wischmeyer, P. E., Role of L-glutamine in critical illness: new insights. *Current opinion in clinical nutrition and metabolic care* **2003**, *6* (2), 217-22.
19. Lin, T.-C.; Chen, Y.-R.; Kensicki, E.; Li, A. Y.-J.; Kong, M.; Li, Y.; Mohny, R. P.; Shen, H.-M.; Stiles, B.; Mizushima, N.; Lin, L.-I.; Ann, D. K., Autophagy: Resetting glutamine-dependent metabolism and oxygen consumption. *Autophagy* **2012**, *8* (10), 1477-1493.
20. Yang, C.; Ko, B.; Hensley, C. T.; Jiang, L.; Wasti, A. T.; Kim, J.; Sudderth, J.; Calvaruso, M. A.; Lumata, L.; Mitsche, M.; Rutter, J.; Merritt, M. E.; DeBerardinis, R. J., Glutamine oxidation maintains the TCA cycle and cell survival during impaired mitochondrial pyruvate transport. *Molecular cell* **2014**, *56* (3), 414-424.
21. Yuneva, M.; Zamboni, N.; Oefner, P.; Sachidanandam, R.; Lazebnik, Y., Deficiency in glutamine but not glucose induces MYC-dependent apoptosis in human cells. *J Cell Biol* **2007**, *178* (1), 93-105.
22. Crespo, J. L.; Powers, T.; Fowler, B.; Hall, M. N., The TOR-controlled transcription activators GLN3, RTG1, and RTG3 are regulated in response to intracellular levels of glutamine. *Proceedings of the National Academy of Sciences of the United States of America* **2002**, *99* (10), 6784-6789.

23. Wise, D. R.; DeBerardinis, R. J.; Mancuso, A.; Sayed, N.; Zhang, X.-Y.; Pfeiffer, H. K.; Nissim, I.; Daikhin, E.; Yudkoff, M.; McMahon, S. B.; Thompson, C. B., Myc regulates a transcriptional program that stimulates mitochondrial glutaminolysis and leads to glutamine addiction. *Proceedings of the National Academy of Sciences* **2008**, *105*, 18782-18787.
24. Gao, P.; Tchernyshyov, I.; Chang, T. C.; Lee, Y. S.; Kita, K.; Ochi, T.; Zeller, K. I.; De Marzo, A. M.; Van Eyk, J. E.; Mendell, J. T.; Dang, C. V., c-Myc suppression of miR-23a/b enhances mitochondrial glutaminase expression and glutamine metabolism. *Nature* **2009**, *458* (7239), 762-5.
25. Nicklin, P.; Bergman, P.; Zhang, B.; Triantafellow, E.; Wang, H.; Nyfeler, B.; Yang, H.; Hild, M.; Kung, C.; Wilson, C.; Myer, V. E.; MacKeigan, J. P.; Porter, J. A.; Wang, Y. K.; Cantley, L. C.; Finan, P. M.; Murphy, L. O., Bidirectional Transport of Amino Acids Regulates mTOR and Autophagy. *Cell* **2009**, *136* (3), 521-534.
26. Smith, R. J., Glutamine metabolism and its physiologic importance. *JPEN. Journal of parenteral and enteral nutrition* **1990**, *14* (4 Suppl), 40s-44s.
27. Bhutia, Y. D.; Ganapathy, V., Glutamine transporters in mammalian cells and their functions in physiology and cancer. *Biochim Biophys Acta* **2016**, *1863* (10), 2531-9.
28. He, L.; Vasiliou, K.; Nebert, D. W., Analysis and update of the human solute carrier (SLC) gene superfamily. *Human Genomics* **2009**, *3* (2), 195.
29. Albers, T.; Marsiglia, W.; Thomas, T.; Gameiro, A.; Grewer, C., Defining substrate and blocker activity of alanine-serine-cysteine transporter 2 (ASCT2) Ligands with Novel Serine Analogs. *Mol Pharmacol* **2012**, *81* (3), 356-65.
30. Scopelliti, A. J.; Font, J.; Vandenberg, R. J.; Boudker, O.; Ryan, R. M., Structural characterisation reveals insights into substrate recognition by the glutamine transporter ASCT2/SLC1A5. *Nat Commun* **2018**, *9* (1), 38.
31. van Geldermalsen, M.; Wang, Q.; Nagarajah, R.; Marshall, A. D.; Thoeng, A.; Gao, D.; Ritchie, W.; Feng, Y.; Bailey, C. G.; Deng, N.; Harvey, K.; Beith, J. M.; Selinger, C. I.; O'Toole, S. A.; Rasko, J. E.; Holst, J., ASCT2/SLC1A5 controls glutamine uptake and tumour growth in triple-negative basal-like breast cancer. *Oncogene* **2016**, *35* (24), 3201-8.

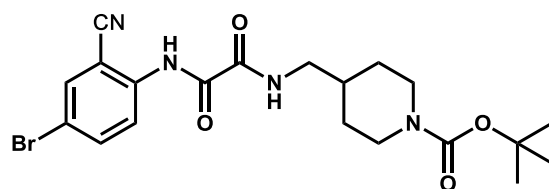
32. Marshall, A. D.; van Geldermalsen, M.; Otte, N. J.; Lum, T.; Vellozzi, M.; Thoeng, A.; Pang, A.; Nagarajah, R.; Zhang, B.; Wang, Q.; Anderson, L.; Rasko, J. E. J.; Holst, J., ASCT2 regulates glutamine uptake and cell growth in endometrial carcinoma. *Oncogenesis* **2017**, *6*, e367.
33. Bobrovnikova-Marjon, E.; Hurov, J. B., Targeting Metabolic Changes in Cancer: Novel Therapeutic Approaches. *Annual Review of Medicine* **2014**, *65* (1), 157-170.
34. Esslinger, C. S.; Cybulski, K. A.; Rhoderick, J. F., Ngamma-aryl glutamine analogues as probes of the ASCT2 neutral amino acid transporter binding site. *Bioorg Med Chem* **2005**, *13* (4), 1111-8.
35. Schulte, M. L.; Dawson, E. S.; Saleh, S. A.; Cuthbertson, M. L.; Manning, H. C., 2-Substituted Ngamma-glutamylanilides as novel probes of ASCT2 with improved potency. *Bioorg Med Chem Lett* **2015**, *25* (1), 113-6.
36. Schulte, M. L.; Khodadadi, A. B.; Cuthbertson, M. L.; Smith, J. A.; Manning, H. C., 2-Amino-4-bis(aryloxybenzyl)aminobutanoic acids: A novel scaffold for inhibition of ASCT2-mediated glutamine transport. *Bioorg Med Chem Lett* **2016**, *26* (3), 1044-7.
37. Schulte, M. L.; Fu, A.; Zhao, P.; Li, J.; Geng, L.; Smith, S. T.; Kondo, J.; Coffey, R. J.; Johnson, M. O.; Rathmell, J. C.; Sharick, J. T.; Skala, M. C.; Smith, J. A.; Berlin, J.; Washington, M. K.; Nickels, M. L.; Manning, H. C., Pharmacological blockade of ASCT2-dependent glutamine transport leads to antitumor efficacy in preclinical models. *Nature Medicine* **2018**, *24*, 194.
38. Schrodinger, L. L. C. *The PyMOL Molecular Graphics System*, Version 1.3r1; 2010.
39. Ma, P.; Deshmukh, Y. S.; Wilsens, C. H. R. M.; Ryan Hansen, M.; Graf, R.; Rastogi, S., Self-assembling process of Oxalamide compounds and their nucleation efficiency in bio-degradable Poly(hydroxyalkanoate)s. *Scientific Reports* **2015**, *5*, 13280.

## Appendix

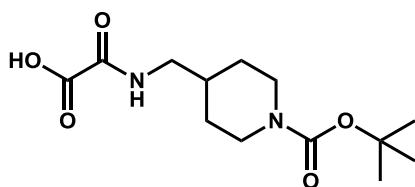
### Lewis Structures: Compounds (3-6f)



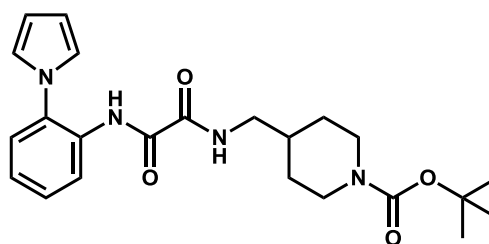
3



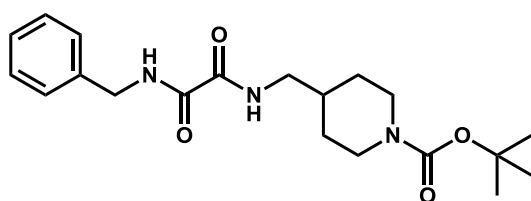
6c



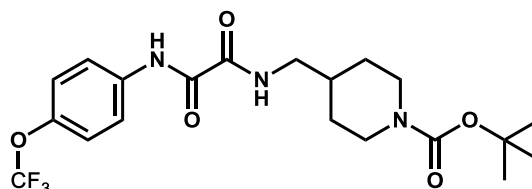
4



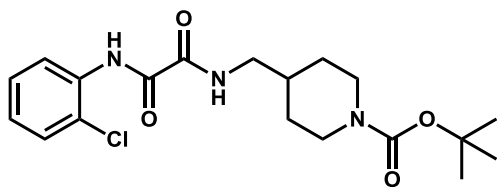
6d



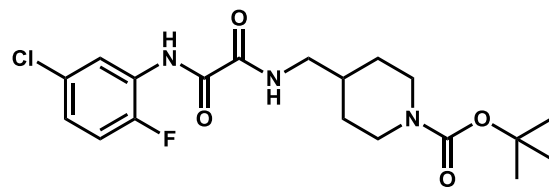
6a



6e



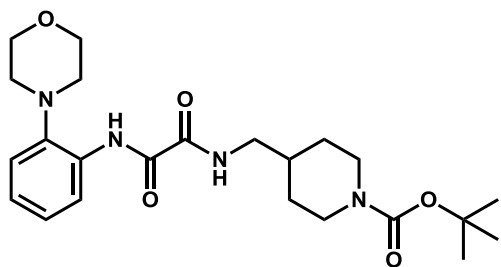
6b



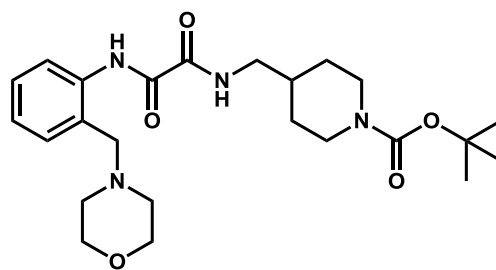
6f



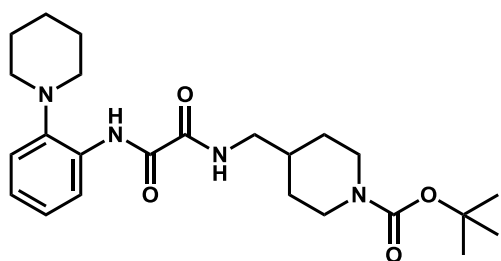
Lewis Structures: Compounds (6g-6n)



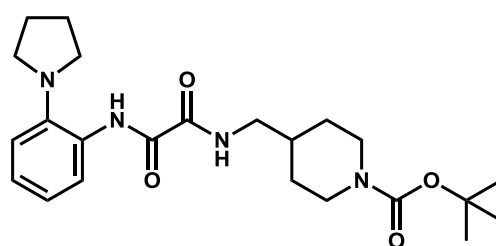
6g



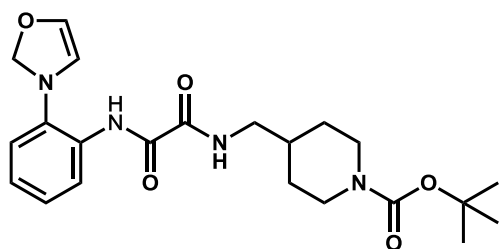
6k



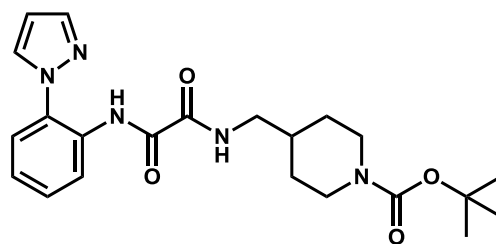
6h



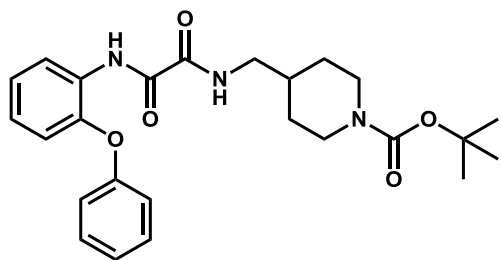
6l



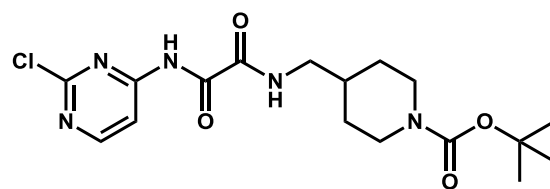
6i



6m

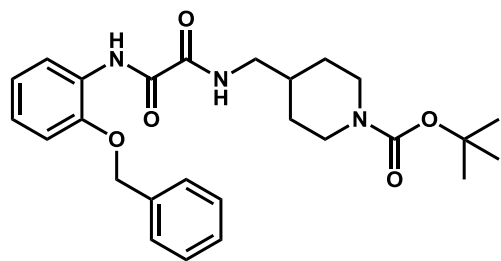


6j

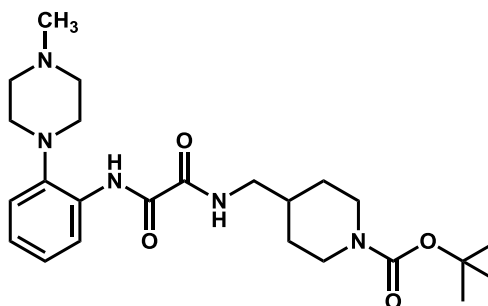


6n

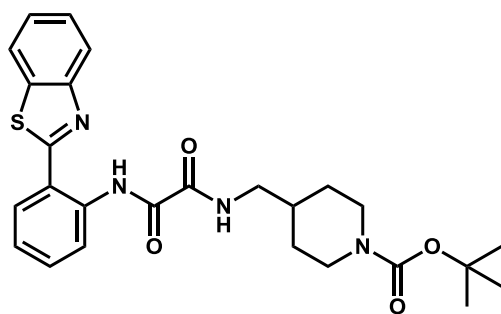
Lewis Structures: Compounds (6o-6v)



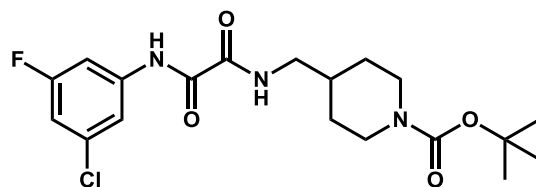
6o



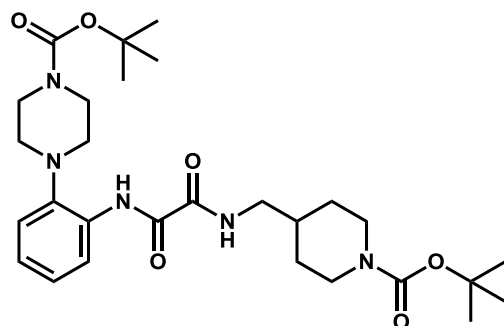
6s



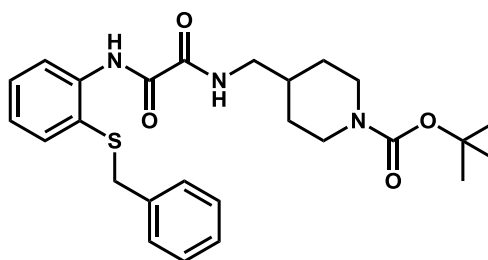
6p



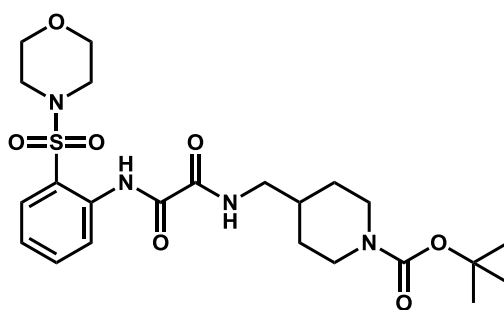
6t



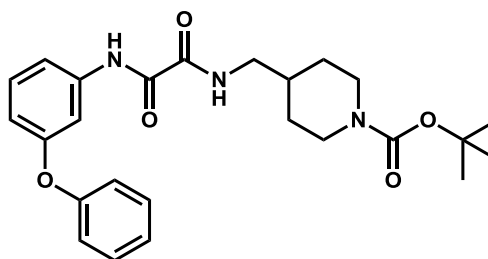
6q



6u

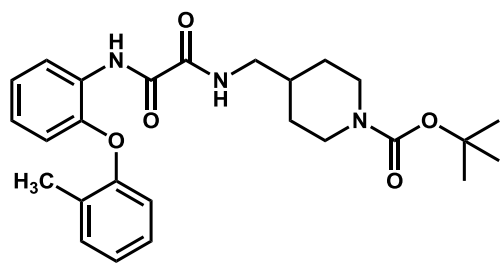


6r

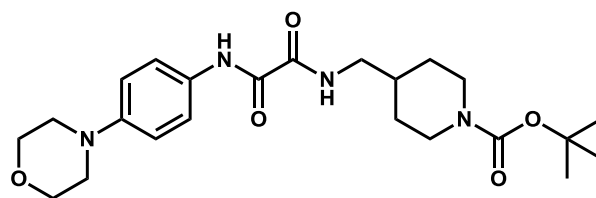


6v

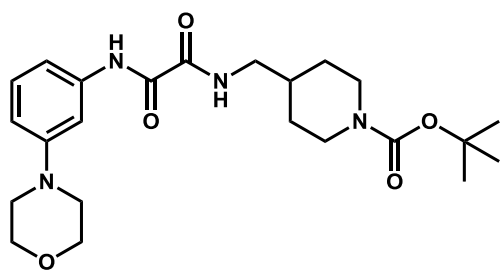
Lewis Structures: Compounds (6w-6y)



6w

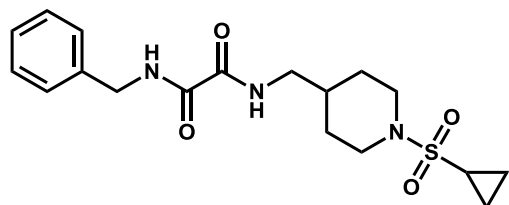


6y

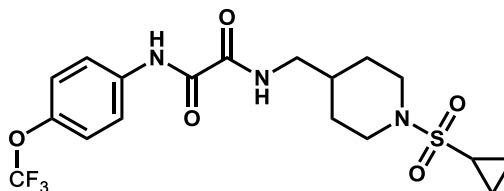


6x

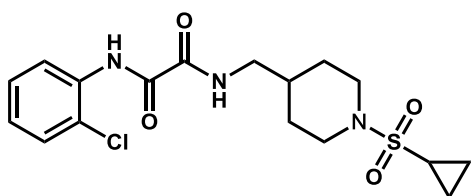
Lewis Structures: Compounds (8a-h)



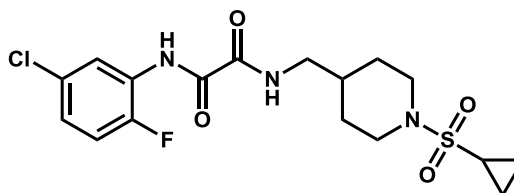
8a



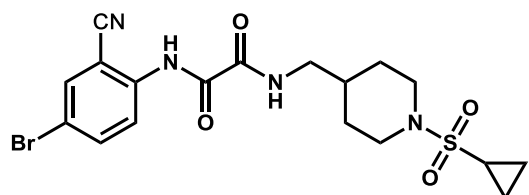
8e



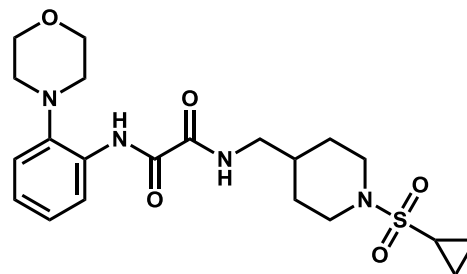
8b



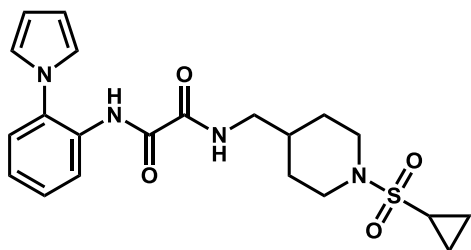
8f



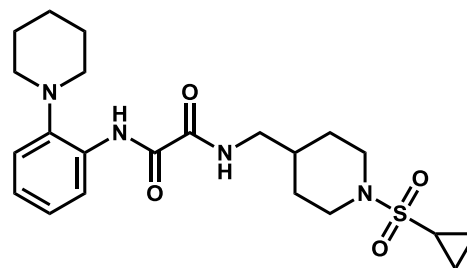
8c



8g

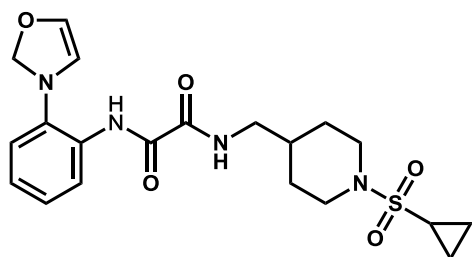


8d

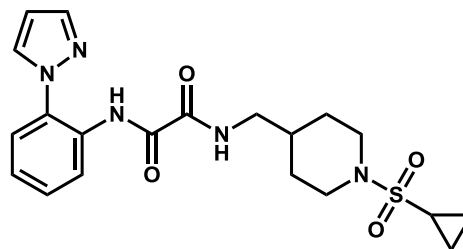


8h

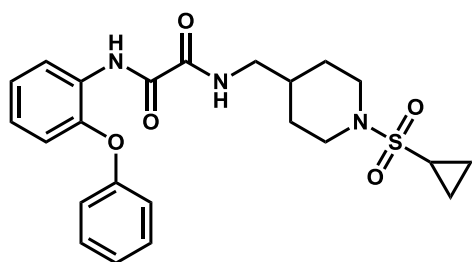
Lewis Structures: Compounds (8i-q)



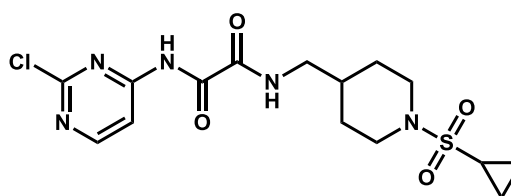
8i



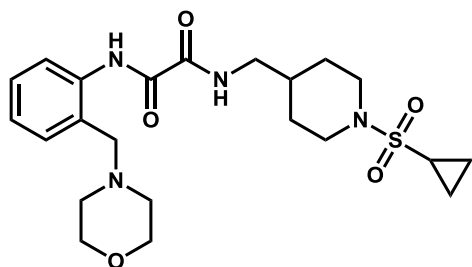
8m



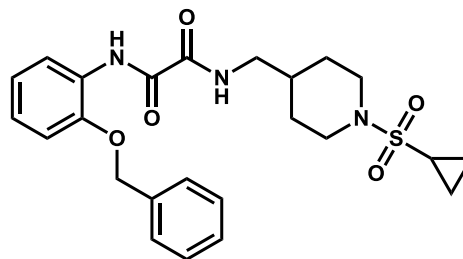
8j



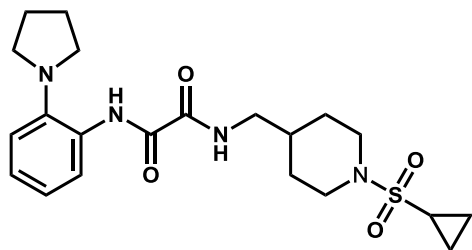
8n



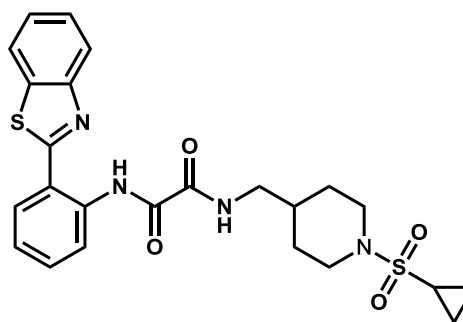
8k



8o

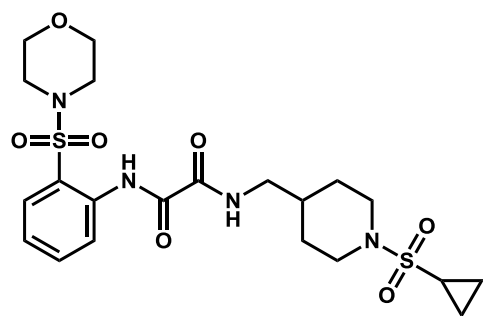


8l

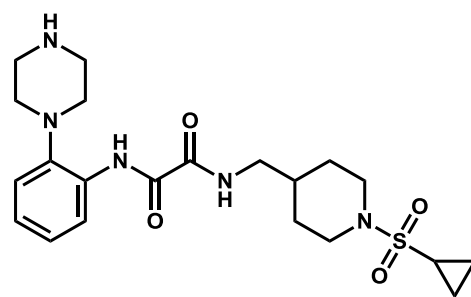


8p

Lewis Structures: Compounds (8q-r)



8q



8r

# NMR Spectra

